Reprinted from

CMC

Computers, Materials, & Continua

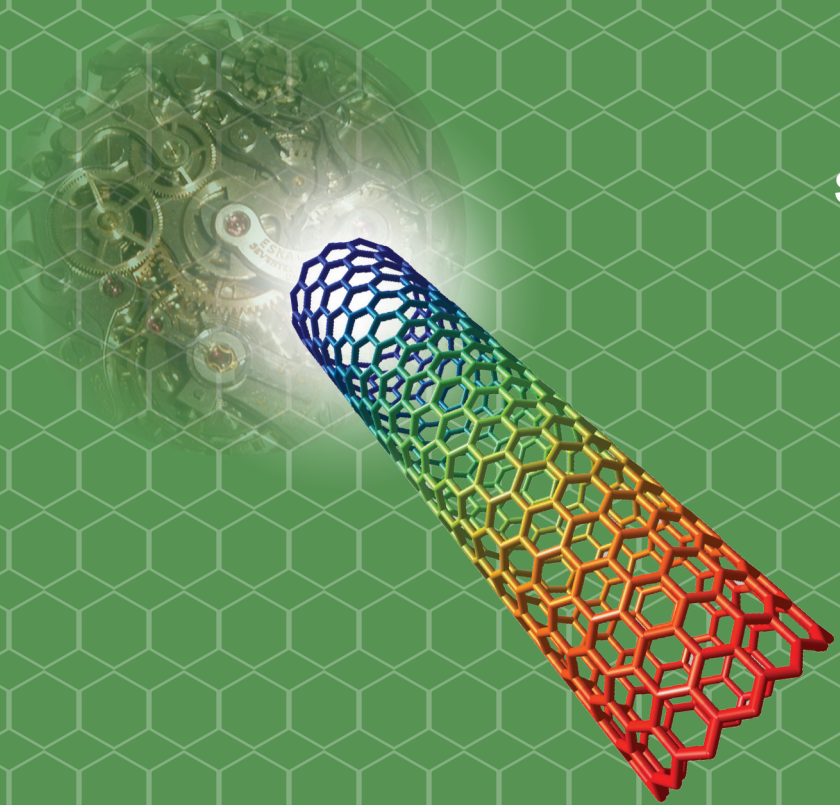

ISSN: 1546-2218 (print)
ISSN: 1546-2226 (on-line)

Tech Science Press

 CMC, vol.14, no.1, pp.23-34, 2009

Nanobubbles at Water-Solid Interfaces: Calculation of the Contact Angle Based on a Simple Model

H. Elnaiem[1] , D. Casimir[1], P. Misra[1] and S.M. Gatica[1,2]

Abstract: Nanobubbles have been found to form at the interface of water and solid surfaces. We examine the conditions for such bubbles to form and estimate the pressure inside the bubble based on thermodynamic considerations. Using a simple model we calculate the contact angle for a wide range of temperatures and hypothetical substrates possessing a continuous range of strengths. We show that as the temperature increases the shape of a bubble changes continuously from a spherical cap with low curvature to a complete sphere. An equivalent effect results from either increasing the strength of the solid or decreasing the surface tension. A model of a substrate formed by layers of materials is proposed to obtain a nanobubble with a particular contact angle.

Keywords: Nanobubbles, liquid-solid interface, contact angle.

1 Introduction

Nanobubbles are tiny gas bubbles that have been observed to form at liquid-solid interfaces. Originally proposed as an explanation for the origin of long-range hydrophobic attractions [Parker, Claesson and Attard, (1994)], their existence was doubted because of predictions that such small bubbles should rapidly dissolve because of the high internal pressure associated with the interfacial curvature and the resulting increase in gas solubility. In recent years, there has been an accumulation of evidence for the existence of nanobubbles at the interface of water and hydrophobic solid surfaces [Zhang, Khan, and Ducker (2007); Tyrrell and Attard (2001); Zhang, Li, Maeda, and Hu (2006)].

Zhang et.al. showed by using a method of solvent exchange that very thin gas phases can exist at the boundary of water and a hydrophobic solid for at least an hour [Zhang, Kahn, and Ducker (2007)]. Using CO_2 for the gas phase, and through

[1] Department of Physics and Astronomy, Howard University, Washington, DC 20059
[2] Corresponding author. sgatica@howard.edu

density measurements of the gas obtained through infrared spectroscopy, the pressure was shown to be approximately atmospheric pressure, accounting for the observed long lifetime of nanobubbles. Tyrell et.al. measured the size of nanobubbles from Atomic Force Microscopy images, finding a height above the substrate of approximately 20 to 30 nm, and a mean area of about $4x10^3$ nm^2 to $6x10^3$ nm^2 [Tyrell and Attard (2001)]. It was also found that the contact angle of water next to nanobubbles on Highly Ordered Pyrolitic Graphite (HOPG) substrates was about twice as large as that for a macroscopic drop on the same substrate [Zhang, Li, Maeda, and Hu (2006)]; specifically, the contact angle for the former was measured at 160 degrees, while the contact angle for the latter was 80 degrees.

The contact angle is a parameter that determines the form and shape of the bubble and depends on the composition of the solid surface and the temperature. In this paper, we use a simple model to calculate the contact angle and show how it is modified by the properties of the material used and the associated temperature.

There have been several relevant studies relating to computer simulation of random sphere packing [Li, Zhao, and Liu (2008)], computational nano-mechanics [Shen and Atluri (2004)], computational studies on mechanical and thermal properties of carbon nanotube based nanostructures [Chakrabarty and Cagin (2008)], and multiscale nonlinear constitutive modeling of carbon nanostructures based on interatomic potentials [Ghanbari and Naghdabadi (2009)], that have provided insight into the understanding of interactions at the interface of water and solid surfaces and aided modeling of substrates formed by layers of materials.

The present paper is organized as follows. The equilibrium properties and parameters of the nanobubbles are described in Section 2. In Section 3 we discuss the simple model and the results of our calculation of the contact angle. Section 4 summarizes the results and presents the conclusions reached based on our model.

2 Nanobubbles

In Fig. 1 we represent schematically a bubble on a solid flat surface. The radius of curvature, R_c, is larger than the actual radius of the bubble (r), and is given by

$$R_c = \frac{r}{\sin(\theta)} \tag{1}$$

where θ is the contact angle at the gas-liquid-solid interface. The contact angle is zero when the liquid wets the solid, and 180^o in the opposite situation, usually termed "non-wetting".

The volume of the bubble is given by

$$V = \frac{4}{3}\pi R_c^3 f(\theta) \tag{2}$$

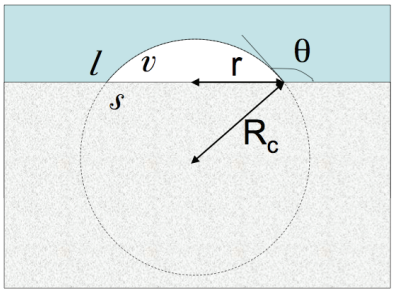

Figure 1: Schematic view of a nanobubble (white) in water (light blue) supported by a flat solid material (grey). The dashed line represents the sphere that contains the bubble.

with

$$f(\theta) = \tfrac{1}{2}\left(1+\cos(\theta)\right) + \tfrac{1}{4}\left(\cos(\theta)\sin(\theta)^2\right) \tag{3}$$

For a spherical (not-supported) bubble of radius R, the excess pressure of the vapor inside the bubble with respect to the pressure of the liquid is given by the Young-Laplace equation

$$\Delta P = \frac{2\sigma_{vl}}{R} \tag{4}$$

where σ_{vl} is the surface tension at the vapor-liquid interface. For a bubble supported by a solid surface, as in Fig. 1, the excess pressure follows the same law with R replaced by the radius of curvature, R_c. If we compare two bubbles of the same volume, one free and the other supported, the excess pressure is smaller in the latter case, and the ratio is given by

$$\frac{\Delta P}{\Delta P_{free}} = [f(\theta)]^{1/3} \tag{5}$$

This pressure ratio is shown in Fig. 2 as a function of the contact angle.

Notice that for a completely non-wetting (θ = 180^o) situation, the bubble becomes a flat film of vapor that has zero excess pressure. In the opposite limit of complete wetting, the supported and free bubbles are actually identical.

The value of the contact angle depends on a delicate balance between the adsorption energy and the cohesive energy within the film. Thus, a quantitative understanding of the properties at the interface requires knowledge of these very weak

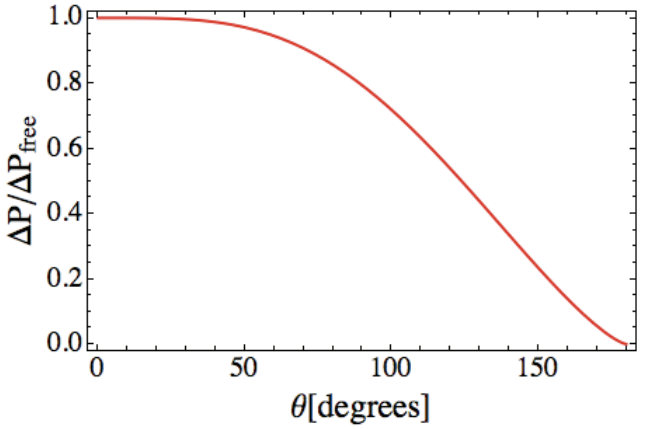

Figure 2: Ratio of the excess pressure of the supported bubble relative to a free bubble of the same volume and at the same temperature.

interactions. This indeed presents a challenge to our understanding of electronic properties at surfaces, which is especially difficult because of the van der Waals interactions responsible for the attraction involving the nonlocal correlation energy-the weak, dynamical coupling between charge fluctuations of the adatom and the solid.

3 Contact Angle of Water on Solid Surfaces

The well-known Young's equation, provides the relationship between the contact angle θ and the three surface tensions σ_{sv}, σ_{lv} and σ_{sl}at the solid-vapor, liquid-vapor and solid-liquid interfaces, respectively:

$$\sigma_{sv} = \sigma_{lv}\cos(\theta) + \sigma_{sl} \tag{6}$$

See Fig. 1 for a schematic representation of the three interfaces.

Eq. 6 is usually applied to the study of wetting transitions. The general subject of wetting has been reviewed in a number of places [Cheng, Cole, Dupont-Roc, Saam, and Treiner

(1993); Phillips, Taborek, and Rutledge (1998); McMillan, Rutledge, and Taborek (2005); Hallock (1995); Rauscher and Dietrich (2008); Gatica and Cole (2009)]. The low temperature wetting properties of the inert gases and H_2 are relatively well understood based on first principle calculations; however, other liquids are

either not understood theoretically or have yet to have the relevant predictions tested experimentally.

The contact angle may be estimated from Eq. 6 given the values of the three surface tensions. Unfortunately, only σ_{lv} is known in some cases. While computer simulation is usually the theoretical tool of choice for quantitative calculations of the interface properties, one would like to have a more convenient method to calculate the contact angle. We have found useful a so-called "simple model" [Cheng, Cole, Saam, and Treiner (1991, 1992, 1993); Chizmeshya, Cole, and Zaremba (1998); Curtarolo, Stan, Bojan, Cole, and Steele (2000); Gatica, Johnson, Zhao, and Cole (2004)] in which one approximates the solid-liquid (s-l) interfacial tension as follows:

$$\sigma_{sl} \approx \sigma_{sv} + \sigma_{lv} + \rho_l \int dz V(z) \tag{7}$$

Here, V(z) is the adsorption potential that is taken to be a function of just the surface-normal distance, z; which is a reasonable approximation to the weakly attractive potentials responsible for the nonwetting behavior at low T, since the adsorbed atom lies far from the surface atoms. The right-most term in Eq. 7 approximates the gas-surface interaction energy in terms of the bulk liquid density, ρ_l, and the integral between the minimum in the adsorption potential at $z = z_{min}$ and $z = \infty$. The physical content of Eq. 7 is that the total free energy cost of the s-l interface (σ_{sl}) equals that of terminating the solid (σ_{sv}) plus that of terminating the liquid (σ_{lv}), with a "correction" represented by the last term due to the solid-liquid interaction energy. Using Eqs. 6 and 7, the contact angle becomes

$$\cos(\theta) = \frac{(\sigma_{sv} - \sigma_{sl})}{\sigma_{lv}} = -1 - \left(\frac{\rho_l}{\sigma_{lv}}\right) \int dz V(z). \tag{8}$$

Eq. 8 has to be interpreted keeping in mind that the potential V(z) is negative for the range of integration. Thus, in the case of an extremely weak potential V(z) ~ 0, the contact angle is $\theta = 180^0$. Now suppose that - keeping the temperature T constant - the intensity of the substrate energy is slowly increased, then the last term increases in magnitude (but is negative), and hence the contact angle slowly decreases. When the interaction reaches a critical value, such that the last term (ρ_l / σ_{lv}) $\int$dz V(z) = -2, the contact angle becomes exactly zero, and the bubble is a full sphere. If the intensity of the interaction further increases, Eq. 8 is no longer valid; however, the contact angle remains zero. An analogous process can be driven, for example, either by increasing the ratio ρ_l / σ_{lv} by altering the composition of the liquid, or by increasing the temperature.

In this work we use Eq. 8 to calculate the contact angle of water on various substrates of increasing strength. The situation can be realized by a substrate composed

of layers of different materials. Changing the composition and thickness of the layers, the intensity of the potential can be "tuned".

One model of the atom-solid potential that has been used extensively to study adsorption or wetting properties is the "3-9 potential" given by the expression

$$V(z) = \frac{4C^3}{27D^2 z^9} - \frac{C}{z^3} \tag{9}$$

This potential is analogous to the Lennard-Jones 6-12 interatomic potential and is usually adopted for similar reasons. It combines a rigorously correct form of the asymptotic attraction ($V \approx$ - C/z^3) and a simple power law repulsion to yield a qualitatively plausible and mathematically convenient functional form. The constant D represents the well- depth of the potential, which takes the minimum value at z_{min} = $[2C/(3D)]^{1/3}$. By adding layers of a different material to the surface of the solid, the value of the parameter D is changed, while C is kept unmodified, and is determined by the composition of the solid. Using Eq. 9, the integral in Eq. 8 becomes

$$I = -\int dz V(z) = \frac{11}{24}\left(\frac{3}{2}\right)^{2/3}\left(CD^2\right)^{1/3} \tag{10}$$

which, in turn, yields the contact angle

$$\cos(\theta) = -1 + \left(\frac{\rho_l}{\sigma_{lv}}\right) I \tag{11}$$

In this simple model, the integral I in Eq. 10 contains the information about the substrate, while the multiplicative factor (ρ_l/σ_{lv}) depends both on the liquid-vapor composition and the temperature. In Fig. 3 we show the results of our calculation of the contact angle as a function of temperature for water on different surfaces with parameters C = 1075 meV Å^{3}and D = 100 meV, values that correspond to the case of graphite, and hypothetical materials with the same C and D = 200 and 300 meV, respectively.

The contact angle is finite, and hence the bubble is a spherical cap, while T is lower than a certain value called the "wetting temperature", T_w. For T > T_w, the bubble is a full sphere, with zero contact angle. Below T_w, the contact angle increases with decreasing temperature. For example, a spherical bubble that forms on the water-graphite interface at T∼500K, would evolve to a semispherical ($\theta = 90^o$) shape when it cools down to room temperature. Of course, the system has to be maintained at the liquid-vapor equilibrium pressure during the process. As we see in Fig. 3, the value of T_w strongly depends on the parameter D of the substrate potential. T_w indeed decreases with increasing D, meaning that a stronger substrate

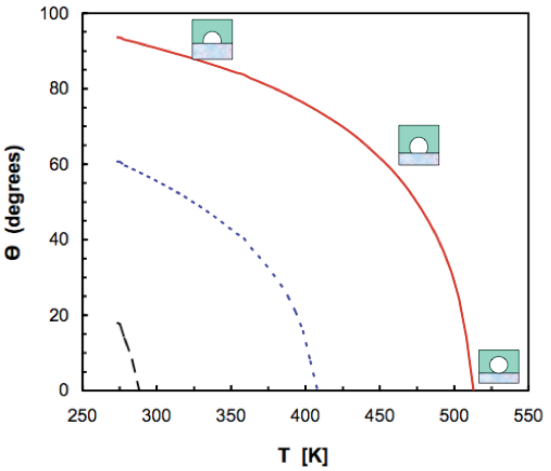

Figure 3: Contact angle for water on various surfaces with parameters C=1074 meV Å^3 and D=100 meV (red solid line), 200 meV (blue dashed line) and 300 meV (black short-dashed line). The inset represents a schematic illustration of the variation in the shape of the bubble as a function of contact angle and temperature.

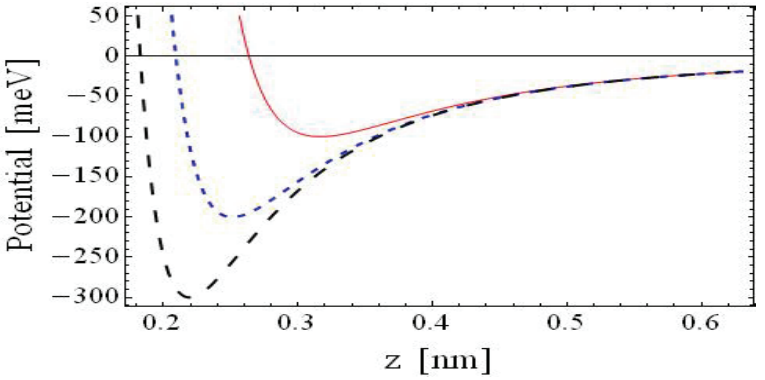

Figure 4: Potentials used in Fig. 3.

"favors" the formation of spherical bubbles at lower temperatures. The three potentials used in generating Fig. 3 are shown in Fig. 4. In Fig. 5 we plot the contact angle as a function of both C and D at room temperature.

This figure provides a hint of how a material can be designed to favor or disfavor the formation of bubbles by modifying the contact angle. As mentioned above, the

parameter D depends on the superficial layers while C is given by the bulk solid material. For example, the values of C for water on graphite, BN, Al, Au and LiF are 1074, 678, 1444, 1644 and 562 meVÅ^3, respectively [Gatica, Johnson, Zhao, and Cole (2004)]. Therefore, adding a graphite layer on the last four bulk solid materials would result in moving our system horizontally through Fig. 5 at D = 100 meV. Another possibility would be to add different layers on top of the same solid, thus moving vertically in the diagram.

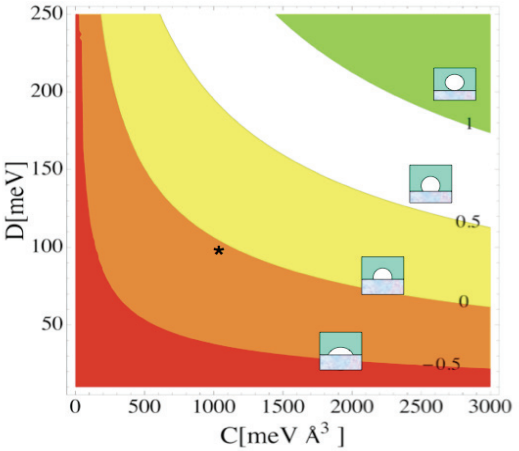

Figure 5: Contour plot of the contact angle θ for water on a solid surface at room temperature as a function of the parameters of the potential, D and C. The inset labels indicate the values of cos[θ]; the star marks the C, D values of the water-graphite potential; and the inset diagrams show various aspects of the bubble. The contact angle is exactly zero in the upper right green zone.

The values of the contact angle displayed in Fig. 5 would be significantly affected by modifications in the density and/or surface tension. In Fig. 6, we show the same diagram for values of the ratio ρ_l/σ_{lv} 20% lower or higher than the value for pure water at room temperature. As we can see in Fig. 6, for example, moving from a) to b), on increasing the temperature, the star indicating graphite moves from the middle portion of the orange zone to the middle portion of the yellow zone.

Typical size of nanobubbles observed at water-solid interfaces are reported to be as small as r = 150 nm - with a contact angle of around 150^o. With these values, the radius of curvature that results from Eq. 1 is R$_c$= 300 nm, which gives an excess pressure of $\sim$ 4.7 atm. Such a bubble would require a large amount of energy to form, and it would be unstable. However, the bubbles are observed to be stable for

many hours. A possible explanation of this stability could be either that the shape is not really spherical, but has a flat top, or that the surface tension is significantly reduced. Another possible solution to this problem, as proposed by Agrawal, is to question the applicability of the Laplace-Young equation in its current form to the phenomena of nanobubbles [Agrawal (2005)]. To justify his argument, he used experimental values for the pressure, volume and temperature of a typical nanobubble, obtained through the use of Atomic Force Microscopy, then calculated the number of gas molecules inside a nanobubble, by assuming the air inside to have an ideal gas equation of state $P_{in}V_b = Nk_BT$. The number of molecules this author calculated for the given experimental values of P, V, and T, were approximately 20,000 molecules. He next calculated the mean free path, λ, which is the distance traveled by a particle before it collides with another one, using the expression where the diameter of an air molecule is d and n is the number of molecules per unit volume. From the experimental values the calculated mean free path was 20-30 nm. Therefore, using the fact that the calculated mean free path has dimensions of the order of the nanobubble itself, it was concluded that the macroscopic definition of pressure does not apply to the phenomena of nanobubbles. The dimensions of interest need to be much larger than the square of the mean free path in order for pressure to be a continuous macroscopic property.

$$\lambda = \frac{1}{\sqrt{2}\,\pi\, d^2\, n} \tag{12}$$

Computer simulations would be required to further study these systems and to check the validity of the models on the nanoscale.

4 Summary and Conclusions

We have presented calculations for the contact angle of nanobubbles formed at a water-solid interface. The results are based on a simple model that relates the contact angle to the surface tension and the water-solid potential. The simplicity of the model allowed us to have a wide view of the dependence of the contact angle on a variety of conditions, including the strength of the potential, the temperature and surface tension.

We have shown that as the temperature increases, the shape of a bubble changes continuously from a spherical cap with low curvature to a complete sphere. An equivalent effect results from either increasing the strength of the solid or decreasing the surface tension.

Improvements to the potential used in the present work and rigorous computer simulations would be needed to conduct a more precise study. Although fairly accurate

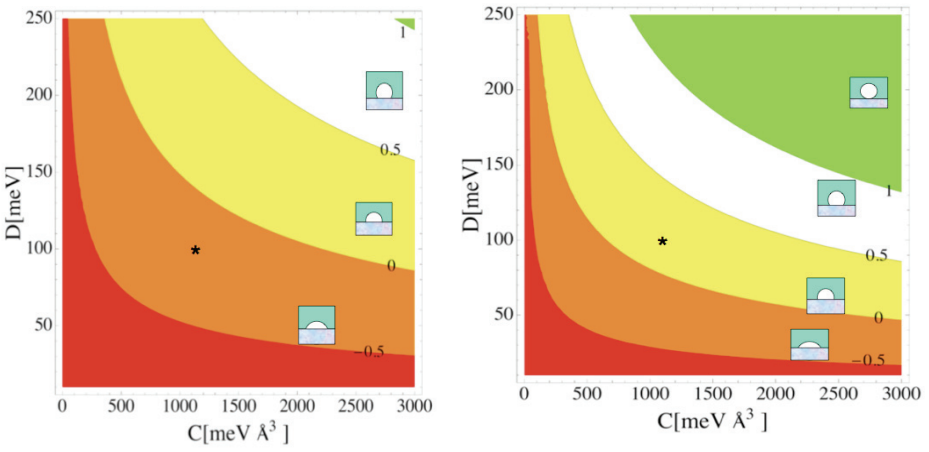

Figure 6: Same as Fig. 5 for values of ρ_l/σ_{lv} 20% lower (a) and 20% higher (b) than the value for pure water at room temperature.

models for the interaction of water on graphite are available [Zhao and Johnson (2005)], that is not the case for most other liquid-solid interfaces, where the force fields would have to be obtained from *ab initio* methods, such as the Density Functional theory.

Acknowledgement: Financial support from the Howard University Fund for Academic Excellence Grant Program is gratefully acknowledged.

References

Agrawal, A. (2005): *An experimental study of nanobubbles on hydrophobic surfaces.* Master's Thesis, Massachusetts Institute of Technology.

Chakrabarty, A.; Cagin, T. (2008): Computational studies on mechanical and thermal properties of carbon nanotube based nanostructures. *CMC: Computers, Materials & Continua,* vol. 7, No. 3, pp. 167-190.

Cheng, E.; Cole, M.W.; Dupont-Roc, J.; Saam, W.F.; Treiner, J. (1993): Novel wetting behavior in quantum films. *Rev. Mod. Phys.,* vol. 65, pp. 557-567.

Cheng, E.; Cole, M. W.; Saam, W. F.; Treiner, J. (1993): Wetting transitions of classical liquid films: a nearly universal trend. *Phys. Rev.,* vol. B48, pp. 18214-18221.

Chizmeshya, A.; Cole, M. W.; Zaremba, E. (1998): Weak binding potentials and wetting transitions. *J. Low Temp. Phys.,* vol. 110, pp. 677-684.

Curtarolo, S.; Stan, G.; Bojan, M. J.; Cole, M. W.; Steele, W. A. (2000): Threshold for wetting at the triple point. *Phys. Rev. E,* vol. 61, pp. 1670-1675

Gatica, S.M.; Johnson, J.K.; Zhao, X.C.; Cole, M.W. (2004): Wetting transition of water on graphite and other surfaces. *Journal of Physical Chemistry B.,* vol. 108, pp. 11704-11708.

Gatica, S.M.; Cole, M.W. (2009): To wet or not to wet: that is the question. *J. Low Temp. Phys.*, in press.

Ghanbari, J.; Naghdabadi, R. (2009): Multiscale nonlinear constitutive modeling of carbon nanostructures based on interatomic potentials. *CMC: Computers, Materials & Continua,* vol. 10, No. 1, pp. 41-64.

Hallock, R.B. (1995): Review of some of the experimental evidence for the novel wetting of helium on alkali metals. *J. Low Temp. Phys.,* vol. 101, pp. 31-40.

Li, S.X.; Zhao, L.; Liu, Y.W. (2008): Computer simulation of random sphere packing in an arbitrarily shaped container. *CMC: Computers, Materials & Continua,* vol. 7, No. 2, pp. 109-118.

McMillan, T.; Rutledge, J.E.; Taborek, P. (2005): Ellipsometry of liquid helium films on gold, cesium and graphite. *J. Low Temp. Phys.*, vol. 138, pp. 995-1011.

Parker, J.L.; Claesson, P. M.; Attard, P. (1994): Bubbles, cavities, and the long-ranged attraction between hydrophobic surfaces. *Journal of Physical Chemistry*, vol. 98, pp 8468-8480.

Phillips, J.A.; Taborek, P.; Rutledge, J.E. (1998): Experimental survey of wetting and superfluid onset of 4He on alkali metal surfaces. *J. Low Temp. Phys.,* vol. 113, pp. 829-834.

Rauscher, M.; Dietrich, S. (2008): Wetting phenomena in nanofluidics. *Ann. Rev. Mat. Rsch.,* vol. 38, pp. 143-172.

Shen, S.; Atluri, S.N. (2004): Computational nano-mechanics and multi-scale simulation. *CMC: Computers, Materials & Continua,* vol. 1, No. 1, pp. 59-90.

Tyrell, J. W. G.; Attard, P. (2001)**:** Images of nanobubbles on hydrophobic surfaces and their interactions. *Physical Review Letters,* vol. 87, no. 17, pp. 176104-1 – 176104 – 4.

Zhang, X.H.; Li, G.; Maeda, N.; Hu, J. (2006): Removal of induced nanobubbles from water/graphite interfaces by partial degassing. *Langmuir,* vol. 22, pp. 9238 – 9243.

Zhang, X.H.; Kahn, A.; Ducker, W. (2007): A nanoscale gas state. *Physical*

Review Letters, vol. 98, pp. 136101-1 – 136101-4.

Zhao, X.C.; Johnson, J.K. (2005): An effective potential of adsorption of polar molecules on graphite. *Molecular Simulations*, vol. 31, pp 1-10.

CMC: Computers, Materials, & Continua

ISSN: 1546-2218 (Print); 1546-2226(Online)

Journal website:
http://www.techscience.com/cmc/

Manuscript submission
http://submission.techscience.com

Published by
Tech Science Press
5805 State Bridge Rd, Suite G108
Duluth, GA 30097-8220, USA

Phone (+1) 678-392-3292
Fax (+1) 678-922-2259
Email: sale@techscience.com
Website: http://www.techscience.com
Subscription: http://order.techscience.com

CMC is Indexed & Abstracted in
Applied Mechanics Reviews; Cambridge Scientific Abstracts (Aerospace and High Technology; Materials Sciences & Engineering; and Computer & Information Systems Abstracts Database); Engineering Index (EMBASE, Compendex, Geobase and Scopus, SecienceDirect Navigator); INSPEC Databases; Mechanics; Science Citation Index; Science Navigator; Zentralblatt fur Mathematik.